

Migration of dynamic subsidence across the Late Cretaceous United States Western Interior Basin in response to Farallon plate subduction

Shaofeng Liu¹, Dag Nummedal², and Lijun Liu³

¹State Key Laboratory of Geological Processes and Mineral Resources, China University of Geosciences (Beijing), Beijing 100083, China

²Colorado Energy Research Institute, Colorado School of Mines, Golden, Colorado 80401, USA

³Institute of Geophysics and Planetary Physics, Scripps Institution of Oceanography, University of California–San Diego, La Jolla, California 92093, USA

ABSTRACT

Backstripped cross sections of the Late Cretaceous succession across central Utah, Colorado, and southern Wyoming in the Western Interior Basin, United States, reveal a component of continuously evolving long-wavelength residual subsidence, in addition to subsidence driven by the Sevier thrust belt and associated sediment loads. The loci of maximum rates of this residual subsidence moved eastward from ca. 98 to 74 Ma in phase with the west to east passage of the Farallon slab, as reconstructed from tomography based on quantitative inverse models. These new subsidence data allow testing of existing subduction models and confirm the dynamic subsidence origin of the Western Interior Basin. Furthermore, regional variations in subsidence rates suggest a possible deficit of negative buoyancy (mantle loading) inside the slab beneath Colorado, supporting the hypothesis that the thickened slab represents a subducted oceanic plateau. This paper documents how the Cretaceous stratigraphy records the timing, patterns, and position of underlying mantle processes during Farallon slab subduction. The new data also reveal patterns indicative of the commencement of the Laramide orogeny in the western United States.

INTRODUCTION

The United States Cretaceous Western Interior Basin (Fig. 1) contains an asymmetric sedimentary wedge that thickens westward toward the Cretaceous Sevier fold-and-thrust belt (Cross, 1986; DeCelles, 1994), and has long been viewed as a foreland basin associated with shortening in the thrust belt. However, flexural backstripping studies (Pang and Nummedal, 1995; Liu and Nummedal, 2004) document that subsidence was driven by the load of the Sevier fold-and-thrust belt only within a narrow 120–180 km band directly east of the thrust belt. Most of the Western Interior Basin subsidence appears to have formed in response to mantle flow effects associated with Farallon plate subduction; several different configurations of subduction have been proposed (e.g., Mitrovica et al., 1989; Gurnis, 1992; Burgess and Moresi, 1999; Liu et al., 2008). Due to a lack of quantified dynamic components in earlier subsidence data, these interpretations have been difficult to prove until now. Our new subsidence data based on flexurally backstripped cross sections of the central Rocky Mountains have sufficient temporal and spatial resolution to test proposed subduction models, and reveal how the Cretaceous stratigraphy records the timing, patterns, and position of underlying mantle processes during Farallon subduction.

RESIDUAL OR DYNAMIC SUBSIDENCE BACKSTRIPPED FROM LATE CRETACEOUS STRATA

Late Cretaceous strata of the Western Interior Basin are well suited for quantitative subsidence studies because of precise chronostratigraphic knowledge (e.g., Weimer, 1983; Fouch et al., 1983; Dyman et al., 1994; Hettinger and Kirschbaum, 2002). We have constructed two regional cross sections from well logs penetrating the entire Late Cretaceous succession.

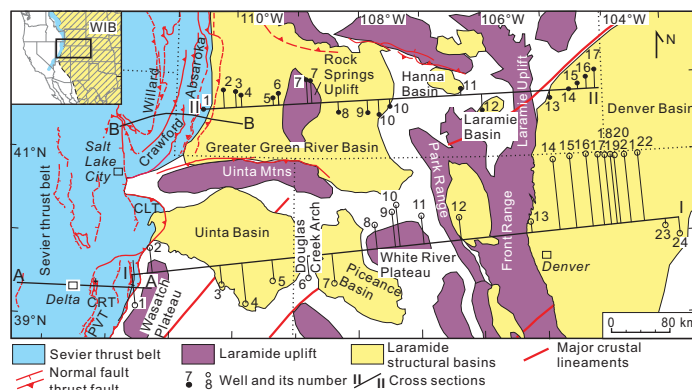


Figure 1. Segment of Sevier thrust belt and its associated basins in central Rocky Mountain area of United States, showing locations of I-I and II-II (Utah–Colorado and Wyoming stratigraphic sections), and A-A and B-B (structural sections across eastern Sevier thrust belt in central Utah and northern Utah–westernmost Wyoming). CRT—Canyon Range thrust; PVT—Pavant thrust; CLT—Charleston thrust; WIB—Western Interior Basin.

Time-stratigraphic correlations were based on the physical continuity of time-parallel marker beds, such as bentonite beds, limestone tops or bases, and shale markers, all of which generate distinctive and traceable log patterns. The ages are tied to established ammonite biozones and radiometric dates (Gradstein et al., 2004). One section extends across central Utah and Colorado (UT–CO) and the other extends across southern Wyoming (WY) (Fig. 1; Tables DR1 and DR2 in the GSA Data Repository¹). The regional stratigraphic correlations along the UT–CO section (Fig. 2), and the sequential restoration of the Sevier thrust belt derived from cross sections in DeCelles and Coogan (2006) (A–A section in Fig. 1), allow a precise spatiotemporal subsidence analysis. Decompaction and flexural backstripping of the UT–CO section (Fig. DR2) followed procedures described in Liu and Nummedal (2004) and Liu et al. (2005) (for methods, see the Data Repository). An earlier published WY section (Liu and Nummedal, 2004) (Fig. DR1) is recalculated based on the updated geologic time scale by Gradstein et al. (2004) (Fig. DR3). The difference between the total subsidence and the amount of subsidence attributable to flexural loading of both the restored Sevier thrust belt and the Western Interior Basin sediments deposited in the syntectonic stages is referred to as residual subsidence (Liu and Nummedal, 2004). This residual subsidence across the UT–CO and WY sections (Figs. DR2 and DR3) displays a dominant, long-wavelength (>500 km) component at all times (blue bands in Figs. 3 and 4).

¹GSA Data Repository item 2011177, methods, Tables DR1 and DR2, and Figures DR1–DR3, is available online at www.geosociety.org/pubs/ft2011.htm, or on request from editing@geosociety.org or Documents Secretary, GSA, P.O. Box 9140, Boulder, CO 80301, USA.

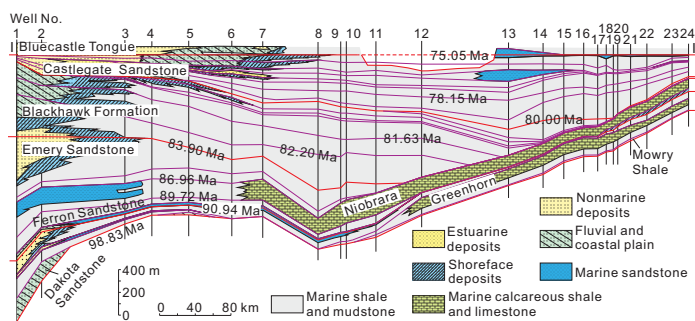


Figure 2. Regional Late Cretaceous stratigraphy across central Utah and Colorado based on 24 well logs along section I-I (in Fig. 1).

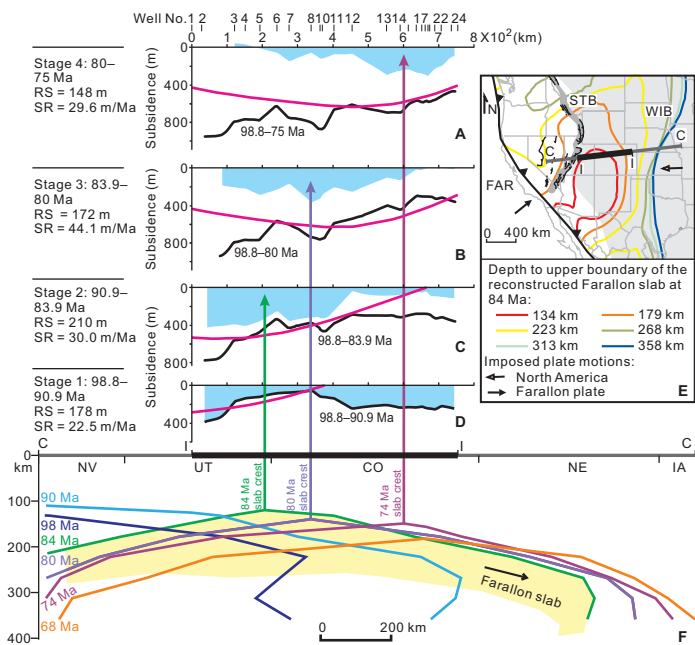


Figure 3. A–D: Profiles of cumulative (black curves) and incremental (blue bands) residual subsidence from backstripped Late Cretaceous strata, with predicted cumulative dynamic subsidence (pink curves) from inverse convection model of Liu et al. (2008), for different time intervals across central Utah and Colorado (section I-I in Fig. 1, heavy dark line in E; RS—incremental residual subsidence averaged over entire profile; SR—averaged incremental subsidence rate). E: Inset map showing main tectonic elements. STB—Sevier thrust belt; WIB—Western Interior Basin (shaded); FAR—Farallon plate. Colored contours indicate depth to upper boundary of reconstructed Farallon slab at 84 Ma, based on isotherms for temperature 32 °C lower than ambient mantle (Liu et al., 2008). F: Calculated upper boundary (colored lines) of modeled Farallon slab at different times (along section line C-C of E) based on inverse convection model (Liu et al., 2008). Modeled slab at 84 Ma is highlighted in yellow. Vertical arrows indicate locations of slab crests through time and space across WIB. NV—Nevada; UT—Utah; CO—Colorado; NE—Nebraska; IA—Iowa.

During the oldest time interval analyzed (98–91 Ma), the residual subsidence was of greatest magnitude along the western margin of the basin and of small magnitude farther east. The high rate of residual subsidence along the western basin margin (~45 m/m.y. in UT-CO and ~85 m/m.y. in WY) overlaps the region of foredeep subsidence related to Sevier thrusting (Figs. 3D and 4D). During the second time interval (91–84 Ma) there was an increase in the overall subsidence rates and an

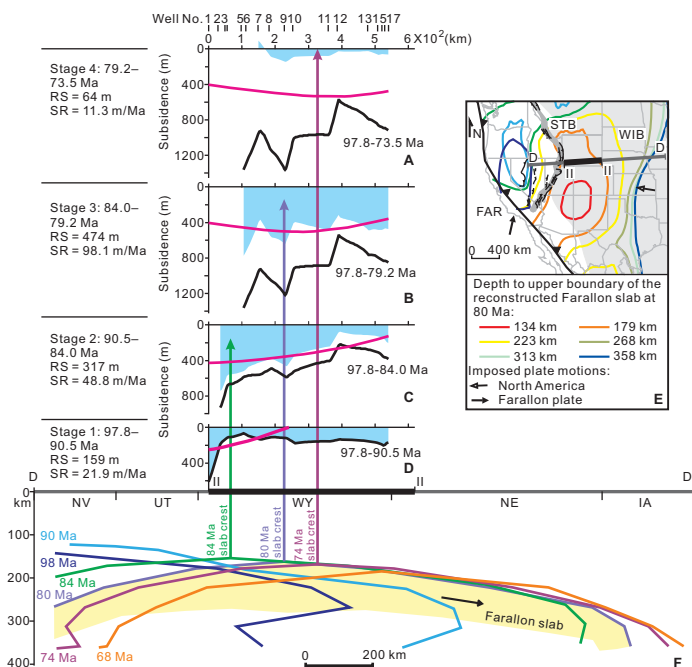


Figure 4. A–D: Profiles of cumulative and incremental residual subsidence from backstripped Late Cretaceous strata, with predicted cumulative dynamic subsidence from inverse convection model, for different time intervals across southern Wyoming (section II-II in Fig. 1, heavy dark line in E). E: Inset map showing main tectonic elements and depth to upper boundary of reconstructed Farallon slab at 80 Ma. F: Calculated upper boundary of modeled Farallon slab at different times (along section line D-D of E). Modeled slab at 80 Ma is highlighted in yellow. WY—Wyoming. Abbreviations as in Figure 3 caption.

eastward extension of the zone of maximum subsidence, while the easternmost parts of the profiles remained flat (Figs. 3C and 4C). During the third time interval (84 to 80 or 79 Ma) the subsidence rates increased by almost 50% in UT-CO (Fig. 3B), and doubled in WY (Fig. 4B). The zone of most rapid subsidence shifted to the middle of the UT-CO profile, whereas the WY section continued to undergo an overall increase in subsidence rate toward the west. To the east of Wyoming, sediments of this age pinch out (Dyman et al., 1994), consistent with a much smaller rate of subsidence there. During the fourth time interval (80 or 79 to 75 or 74 Ma), the overall subsidence rates decreased, most dramatically across the WY section. The center of subsidence along the UT-CO section shifted east to the Denver Basin, where the subsidence rates still remained high (~61 m/m.y.) (Fig. 3A). All along the WY section, the rates of subsidence became very low (~11.3 m/m.y.), with maximum subsidence occurring in the middle of the profile (Fig. 4A).

Overall, the calculated long-wavelength residual subsidence demonstrates a systematic temporal evolution. The magnitude of residual subsidence and its rate, averaged along the entire UT-CO and WY sections, follow a trend of an initial increase to a maximum in mid-life, and a subsequent decrease (Figs. 3 and 4), consistent with a predicted basin formation process by dynamic subsidence (Burgess and Moresi, 1999). Furthermore, the long wavelength of the residual subsidence is also consistent with downward viscous drag caused by a sinking slab (Gurnis, 1992; Gurnis et al., 1998).

PREDICTED DYNAMIC SUBSIDENCE FROM CONVECTION MODELS

The observed cratonward translation of the long-wavelength subsidence across the central Rocky Mountains, characterized by an initial

maximum subsidence in the west and transforming into trough-shaped subsidence profile subsequently (Figs. 3 and 4), permits a rigorous testing of existing geodynamic models. The documented temporal evolution of subsidence suggests that the subducting Farallon plate caused a regionally focused subsidence zone that moved inland with time. Convection models that assume subduction with a fixed geometry of the downgoing slab relative to the overriding plate would generate stationary induced dynamic subsidence patterns (e.g., Mitrović et al., 1989), and thus do not fit our observation. Models that assume gradually shallowing and/or steepening subducting oceanic slabs explain the migration of volcanism across the western United States (Coney and Reynolds, 1977), the continental-scale tilting of North America (Mitrović et al., 1989), and an overall broadening (or narrowing) in the extent of dynamic subsidence as the slab shallows (or steepens), but not the successive landward shift of subsidence centers that is revealed by our backstripped results.

Liu et al. (2008) presented an inverse convection model that both reconstructs the eastward subduction of the Farallon plate and predicts the dynamic subsidence across Northern America since the Late Cretaceous. The cumulative dynamic subsidence predicted by this model (pink curves in Fig. 3) mostly matches our cumulative backstripped residual subsidence (black curves in Fig. 3) across the UT-CO section, both in wavelength and magnitude. Specifically, the backstripped results document an increasing maximum cumulative residual subsidence from 400 to 930 m between 98.8 and 75 Ma with an eastward-migrating depocenter, comparable to the inverse model predictions (Fig. 3). Along the WY section, the inverse model suggests wavelengths and patterns of dynamic subsidence (pink curves in Fig. 4) similar to those of the backstripped cumulative residual one (black curves in Fig. 4) for all four time intervals, but the magnitude of the predicted dynamic subsidence (~500 m) from the inverse model is about half of what is found in the backstripping analysis (~1 km), indicating an inadequacy of the inverse convection model. This is discussed in the following.

DISCUSSION

According to the inverse convection model for Farallon subduction (Liu et al., 2008), a segment of anomalously thick and cool oceanic slab migrated eastward inland beneath North America during the Late Cretaceous (Figs. 3F and 4F). As it moved beneath the continent, the slab had assumed an arched shape with dips in all directions and a fairly distinct crest. The overall negative buoyancy of the sinking Farallon slab caused the surface to subside dynamically. Above the shallow crest of the descending slab, the force of viscous coupling was greater and the dynamic subsidence rate was higher (Richards and Hager, 1984). Due to the westward motion of North America, the leading edge of this slab reached Utah and western Wyoming at 98 Ma and progressively moved inland. The shallow part of the eastward-dipping limb of the slab before 90 Ma caused the high rate of subsidence along the western margin of the study area, and widespread low-magnitude subsidence in the east (Figs. 3D and 4D, stage 1), where the slab was too deep to exert much influence.

As the slab moved farther inland with its crest beneath eastern Utah (Fig. 3F) and western Wyoming (Fig. 4F) at ca. 84 Ma, the entire slab began affecting the Western Interior Basin. Viscous pull by the slab was now at a maximum above the slab crest, at the very western margin of our study area, and was progressively weaker eastward along the slab margin, because of its deepening. The residual subsidence profile at this stage was a mirror image of the eastward dip of the leading edge of the slab (Figs. 3C and 4C, stage 2). The increase in residual subsidence from stages 1–2 reflected the overall shallowing of that part of the slab that was beneath the Western Interior Basin. The residual subsidence center moved to western Colorado (middle Wyoming) at ca. 80 Ma, and the averaged subsidence rates further increased (Figs. 3B and 4B, stage 3), consistent with the model of Liu et al. (2008) that placed the largest areal extent of

shallow slab beneath the Western Interior Basin at that time. The symmetric geometry of the arched slab was a mirror image of the time-correlative trough-shaped subsidence profiles.

After 80 Ma the Farallon plate changed its migration direction with respect to North America from eastward to northeastward, at which time the Farallon slab also sank deeper into the mantle (Liu et al., 2008), overall lessening its viscous pull. Because the bulk of the slab was to the south of Wyoming during most of the Late Cretaceous (Figs. 3E and 4E), the UT-CO section underwent its continued effects, but Wyoming was north of its zone of greatest impact. High subsidence rates in eastern Colorado continued until the end of the Cretaceous (Fig. 3A, stage 4) as the slab crest moved beyond the eastern edge of the state, whereas the residual subsidence in Wyoming essentially came to an earlier end because of the greater depth of the slab there (Fig. 4A, stage 4).

The timing and spatial patterns of subsidence in the Cretaceous Western Interior Basin, documented in Figures 3 and 4, show a correlation with the eastward movement of a Farallon slab with a shallow crest and deepening (and steepening) margins. The physics of slab pull also predict that the rates of subsidence should be inversely related to the depth of the slab surface (with corrections for slab density variations, discussed in the following). Therefore, the observed mirror image of the subsidence profiles and slab crest relief lead us to conclude that the residual subsidence was the dynamic subsidence in nature, and the primary driver behind subsidence in the Western Interior Basin was the dynamic pull of the descending slab.

In reconstructing Farallon plate subduction, Liu et al. (2008) utilized stratigraphic constraints that cover a broad spatial domain with relatively low regional resolution. Therefore, their inferred model represents the simplest solution consistent with these constraints. The broad correlation between the backstripped and predicted regional subsidence in our study, including spatiotemporal migrations (Figs. 3 and 4), provides additional support for the inverse model of Liu et al. (2008). However, the inverse convection model underpredicts dynamic subsidence along the WY section (Fig. 4). Backstripped subsidence rates along the WY section are on average higher than those along the UT-CO section (Figs. 3 and 4), yet the inverse convection model implies that because the slab under the WY section is deeper and thinner than that under the UT-CO section, the negative buoyancy is also smaller, and therefore dynamic subsidence rates along the WY section should be lower. Although the geometry of the localized slab is determined from inverting seismic tomography, its density structure is treated as a simple linear function of seismic anomalies (Liu et al., 2008), potentially ignoring possible regional compositional variations inside the slab. The improved backstripped subsidence with a better resolution both in space and time from the stratigraphic data presented here suggests that the observed larger dynamic subsidence in the WY section may result from lower density in the thickened slab beneath UT-CO. For example, a subducting oceanic plateau (Liu et al., 2010) with thick, lower density crust would provide extra buoyancy below the UT-CO section and could have caused less dynamic subsidence than the normal oceanic slab underlying WY. Moreover, the underpredicted subsidence in WY suggests that the density of the normal Farallon slab is underestimated in the inverse model.

Both the WY and UT-CO profiles for the time interval of 84 to 80 or 79 Ma demonstrate variations in subsidence on a spatial scale of ~100 km, which corresponds to the length scale of the subsequent Laramide basins and ranges. For example, the pronounced peak in the WY profile at Well 7 is at the periphery of the Rock Springs uplift, and the peak at Well 10 is at the periphery of Greater Green River Basin, ~40 km north of the Park Range uplift (Fig. 1). The same correlation occurs on the UT-CO section. Because the slab subduction would cause strong compression in the overriding crust, leading to the development of a number of reverse faults of Laramide age across Wyoming and Colorado (Bird, 1998; Liu et

al., 2010), these short-wavelength peaks in the broad dynamic subsidence profiles may reflect the onset of Laramide-style uplifts at depth. Some of these initial perturbations transformed into surface uplifts after 80 Ma (Figs. 3 and 4, stage 4), when the descending slab moved northeastward and sank deeper into the mantle and the diminished dynamic subsidence caused crustal rebound.

CONCLUSIONS

Quantitative differentiation of subsidence across Utah, Colorado, and Wyoming during the Late Cretaceous reveals that the long-wavelength dynamic subsidence of the Western Interior Basin is characterized by an initial rapid subsidence in the west that subsequently migrated to the east, forming a trough-shaped subsidence profile. The eastward migration of the maximum subsidence zone tracks the passage of the Farallon slab with the shallowest crest. This suggests that the fundamental driver for Western Interior Basin subsidence was the dynamic pull of the sinking slab. Furthermore, the study has also identified a deficit of negative buoyancy (mantle loading) inside the slab to the south of Wyoming, supporting the hypothesis that the thickened slab represents a subducted oceanic plateau. These data also provide insight into the commencement of the Laramide tectonic events in the western United States.

ACKNOWLEDGMENTS

We thank Michael Gurnis for helpful discussions, and Sandra J. Wyld, Michael J. Zaleha, and two other referees for helpful suggestions on the manuscript. This work was supported by Chinese Natural Science Foundation grants (41030318, 40672135, and 40272055), the 111 Project (B07011), Program for Changjiang Scholars and Innovative Research Team in University (IRT0864), Research Partnership to Secure Energy for America (07122-15), Colorado Energy Research Institute at the Colorado School of Mines, ExxonMobil Upstream Research Company, and a Moore Graduate Fellowship at Caltech (L. Liu).

REFERENCES CITED

- Bird, P., 1998, Kinematic history of the Laramide orogeny in latitudes 35°–49°N, western United States: *Tectonics*, v. 17, p. 780–801, doi: 10.1029/98TC02698.
- Burgess, P.M., and Moresi, L.N., 1999, Modelling rates and distribution of subsidence due to dynamic topography over subducting slabs: Is it possible to identify dynamic topography from ancient strata?: *Basin Research*, v. 11, p. 305–314, doi: 10.1046/j.1365-2117.1999.00102.x.
- Coney, P.J., and Reynolds, S.J., 1977, Cordilleran Benioff zones: *Nature*, v. 270, p. 403–406, doi: 10.1038/270403a0.
- Cross, T.A., 1986, Tectonic controls of foreland basin subsidence and Laramide style deformation, western United States, in Allen, P., and Homewood, P., eds., *Foreland basins: International Association of Sedimentologists Special Publication 8*, p. 15–39.
- DeCelles, P.G., 1994, Late Cretaceous–Paleocene synorogenic sedimentation and kinematic history of the Sevier thrust belt, northeast Utah and southwest Wyoming: *Geological Society of America Bulletin*, v. 106, p. 32–56, doi: 10.1130/0016-7606(1994)106<0032:LCPSSA>2.3.CO;2.
- DeCelles, P.G., and Coogan, J.C., 2006, Regional structure and kinematic history of the Sevier fold-and-thrust belt, central Utah: *Geological Society of America Bulletin*, v. 118, p. 841–864, doi: 10.1130/B25759.1.
- Dyman, T.S., Merewether, E.A., Molenaar, C.M., Cobban, W.A., Obradovich, J.D., Weimer, R.J., and Bryant, W.A., 1994, Stratigraphic transects for Cretaceous rocks, Rocky Mountains and Great Plains regions, in Caputo, M.V., et al., eds., *Mesozoic systems of the Rocky Mountain region, USA*: Denver, Colorado, Rocky Mountain Section, SEPM (Society for Sedimentary Geology), p. 365–392.
- Fouch, T.D., Lawton, T.F., Nichols, D.J., Cashion, W.B., and Cobban, W.A., 1983, Patterns and timing of synorogenic sedimentation in Upper Cretaceous rocks of central and northeast Utah, in Reynolds, M.W., and Dolly, E.D., eds., *Mesozoic paleogeography of the west-central United States: Rocky Mountain Paleogeography Symposium 2*: Denver, Colorado, Rocky Mountain Section, SEPM (Society for Sedimentary Geology), p. 305–336.
- Gradstein, F., Ogg, J., and Smith, A., eds., 2004, *A geologic time scale 2004*: Cambridge, Cambridge University Press, 589 p.
- Gurnis, M., 1992, Rapid continental subsidence following the initiation and evolution of subduction: *Science*, v. 255, p. 1556–1558, doi: 10.1126/science.255.5051.1556.
- Gurnis, M., Müller, R.D., and Moresi, L., 1998, Cretaceous vertical motion of Australia and the Australian–Antarctic discordance: *Science*, v. 279, p. 1499–1504, doi: 10.1126/science.279.5356.1499.
- Hettinger, R.D., and Kirschbaum, M.A., 2002, Stratigraphy of the Upper Cretaceous Mancos Shale (upper part) and Mesaverde Group in the southern part of the Uinta and Piceance Basins, Utah and Colorado: *U.S. Geological Survey Geologic Investigations Series I-2764*, 22 p.
- Liu, L., Spasojevic, S., and Gurnis, M., 2008, Reconstructing Farallon plate subduction beneath North America back to the Late Cretaceous: *Science*, v. 322, p. 934–938, doi: 10.1126/science.1162921.
- Liu, L., Gurnis, M., Seton, M., Saleeby, J., Muller, R.D., and Jackson, J.M., 2010, The role of oceanic plateau subduction in the Laramide orogeny: *Nature Geoscience*, v. 3, p. 353–357, doi: 10.1038/ngeo829.
- Liu, S.F., and Nummedal, D., 2004, Late Cretaceous subsidence in Wyoming: Quantifying the dynamic component: *Geology*, v. 32, p. 397–400, doi: 10.1130/G20318.1.
- Liu, S.F., Nummedal, D., Yin, P.G., and Luo, H.J., 2005, Linkage of Sevier thrust episodes and Late Cretaceous megasequences across southern Wyoming (USA): *Basin Research*, v. 17, p. 487–506, doi: 10.1111/j.1365-2117.2005.00277.x.
- Mitrovica, J.X., Beaumont, C., and Jarvis, G.T., 1989, Tilting of continental interiors by the dynamical effects of subduction: *Tectonics*, v. 8, p. 1079–1094, doi: 10.1029/TC008i005p01079.
- Pang, M., and Nummedal, D., 1995, Flexural subsidence and basement tectonics of the Cretaceous Western Interior basin, United States: *Geology*, v. 23, p. 173–176, doi: 10.1130/0091-7613(1995)023<0173:FSABTO>2.3.CO;2.
- Richards, M.A., and Hager, B.H., 1984, Geoid anomalies in a dynamic Earth: *Journal of Geophysical Research*, v. 89, p. 5987–6002, doi: 10.1029/JB089iB07p05987.
- Weimer, R.J., 1983, Relation of unconformities, tectonics, and sea level changes, Cretaceous of the Denver basin and adjacent areas, in Reynolds, M.W., and Dolly, E.D., eds., *Mesozoic paleogeography of the west-central United States: Rocky Mountain Paleogeography Symposium 2*: Denver, Colorado, Rocky Mountain Section SEPM (Society for Sedimentary Geology), p. 359–376.

Manuscript received 24 August 2010

Revised manuscript received 11 January 2011

Manuscript accepted 1 February 2011

Printed in USA